Proceedings of PVP2008
2008 ASME Pressure Vessels and Piping Division Conference
July 21-31, 2008, Chicago, Illinois

PVP2008-61129

A Unified View of Engineering Creep Parameters*

D.R. Eno and G. A. Young — Lockheed Martin Corporation
Schenectady, New York, USA

T.-L. (Sam) Sham — Oak Ridge National Laboratory
Oak Ridge, Tennessee, USA
Email: shamt@ornl.gov

ABSTRACT

Creep data are often analyzed using derived engineering parameters to correlate creep life (either time to rupture, or time to a specified strain) to applied stress and temperature. Commonly used formulations include *Larson-Miller*, *Orr-Sherby-Dorn*, *Manson-Haferd*, and *Manson-Succop* parameterizations. In this paper, it is shown that these parameterizations are all special cases of a common general framework based on a linear statistical model. Recognition of this fact allows for statistically efficient estimation of material model parameters and quantitative statistical comparisons among the various parameterizations in terms of their ability to fit a material database, including assessment of a stress-temperature interaction in creep behavior. This provides a rational basis for choosing the best parameterization to describe a particular material. Furthermore, using the technique of maximum likelihood estimation to estimate model parameters allows for a statistically proper treatment of runouts in a test database via censored data analysis methods, and for construction of probabilistically interpretable upper and lower bounds on creep rate. Comparisons are made to a generalization of the commonly used *Larson-Miller* parameterization (namely, the *Mendelson-Roberts-Manson* parameterization), which is comparable in complexity to the Manson-Haferd parameter, but utilizes a reciprocal temperature dependence. The general framework for analysis of creep data is illustrated with analysis of Alloy 617 and HAYNES® 230® alloy[1] (Alloy 230) test data.

* This paper has been authored by a contractor of the U.S. Government under contract No. DE-AC12-00-SN39357. Accordingly, the U.S. Government retains a non-exclusive, royalty-free license to publish or reproduce the published form of this paper, or allows others to do so, for U.S. Government purposes.

[1] HAYNES and 230 are trademarks of Haynes International, Inc.

1.0 INTRODUCTION

Project Prometheus was initiated to develop a space nuclear/electric reactor system for a wide range of deep space and terrestrial missions. The basic concept was a compact fast reactor coupled with a direct gas Brayton cycle turbine that would drive on-board generators for electrical power. The Jupiter Icy Moon Orbiter (JIMO) mission was selected as the first mission and required operation for up to 15 years. The following represents part of the efforts to support the development of preliminary structural design procedures for pre-conceptual structural component sizing analyses.

Creep data are often analyzed using derived engineering parameters to correlate creep life (either time to rupture, or time to a specified strain) to applied stress and temperature. Commonly used formulations include *Larson-Miller*, *Orr-Sherby-Dorn*, *Manson-Haferd*, and *Manson-Succop* parameterizations. In this paper, it is shown that these parameterizations are all special cases of a common general framework based on a linear statistical model. Recognition of this fact allows for statistically efficient estimation of material model parameters, and quantitative statistical comparisons among the various parameterizations in terms of their ability to fit a material database, including assessment of a stress-temperature interaction in creep behavior. This provides a rational basis for choosing the best parameterization to describe a particular material. Furthermore, using the technique of maximum likelihood estimation to estimate model parameters allows for a statistically proper treatment of runouts in a test database via censored data analysis methods, and for construction of probabilistically interpretable upper and lower bounds on creep rate. Comparisons are made to a generalization of the commonly used *Larson-Miller* parameterization (namely, the *Mendelson-Roberts-Manson* parameterization), which is comparable in complexity to the Manson-Haferd

Copyright © 2008 by ASME

formulation, but with an inverse temperature dependence that is characteristic of many creep mechanisms. The general framework for analysis of creep data is illustrated with analysis of the nickel-chromium Alloys 617 and 230 test data.

1.1 Engineering Creep Parameters

Creep testing of structural alloys typically consists of multiple tests, performed under accelerated conditions covering a range of temperatures and applied stresses. Engineering creep parameters are used for extrapolating accelerated creep test results to the stress and temperature conditions of interest. These parameters relate absolute temperature (denoted herein as T) with time to a specified condition (denoted as t), typically either rupture or 1% strain. Reference 1 provides a concise summary of the four engineering creep formulations considered in this report, namely *Larson-Miller*, *Orr-Sherby-Dorn*, *Manson-Haferd*, and *Manson-Succop*.

In fitting an engineering creep parameter to a database, the data are often first normalized to an "iso-stress" condition; that is, the measured times (t) are adjusted for each temperature included in the experimental matrix to approximate a constant stress condition across the entire database. The temperature effect is then fit in a second step, using the normalized iso-stress data.

The Larson-Miller formulation assumes that a specified point ($1/T$, $\log(t)$) = (0, C) is on every iso-stress line (Figure 1). The slope of each iso-stress line is

$$\frac{\log(t)-(-C)}{\frac{1}{T}-0} = T(\log(t)+C)\,. \qquad [1]$$

Making the additional assumption that the slope is a linear function of $\log(\sigma)$ (or, equivalently, $\log(\sigma)$ is a linear function of the slope) yields:

$$\log(\sigma) = a + b\cdot T(\log(t)+C). \qquad [2]$$

This implies:

$$\log(t) = (-C) + \frac{1}{b}\cdot\left(\frac{1}{T}\right) - \frac{a}{b}\cdot\log(\sigma)\cdot\left(\frac{1}{T}\right). \qquad [3]$$

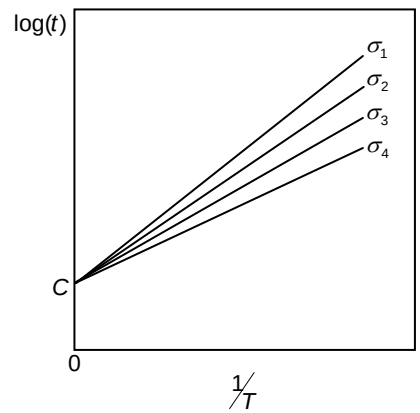

Figure 1. Larson-Miller creep parameterization.

In contrast, the Manson-Haferd formulation assumes that for a fixed stress σ, $\log(t)$ is a linear function of T (vice $1/T$) and that all of the lines go through a common point (T_a, $\log(t_a)$) (Figure 2). So, the slope for a given stress is

$$\frac{\log(t)-\log(t_a)}{T-T_a} \qquad [4]$$

With the additional assumption that the slope is a linear function of $\log(\sigma)$, this becomes:

$$\frac{\log(t)-\log(t_a)}{T-T_a} = a + b\cdot\log(\sigma)\,, \qquad [5]$$

which implies

$$\log(t) = \begin{array}{l}\left(\log(t_a)-a\cdot T_a\right)+a\cdot T \\ -b\cdot T_a\cdot\log(\sigma)+b\cdot T\cdot\log(\sigma)\end{array}. \qquad [6]$$

It can be observed from equations 3 and 6 that while the Larson-Miller approach expresses $\log(t)$ as a linear function of reciprocal temperature, the Manson-Haferd approach expresses $\log(t)$ as a linear function of straight temperature. However, there is another important difference: unlike the Larson-Miller formulation, the Manson-Haferd formulation does not specify that the iso-stress lines intersect at a specific location on the temperature scale. This added flexibility of the Manson-Haferd approach makes it difficult to determine which approach is empirically better for modeling a given material's creep behavior, since the Manson-Haferd formulation may fit a given database better than the Larson-Miller formulation due either to the

Copyright © 2008 by ASME

different temperature form, or the added flexibility, or a combination of the two.

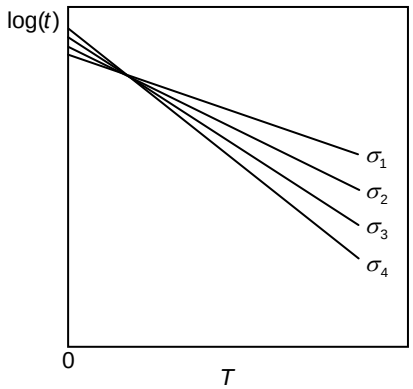

Figure 2. Manson-Haferd creep parameterization.

In the Larson-Miller formulation, the intersection point ($1/T_a$, $\log(t_a)$) could be allowed to be arbitrary rather than fixed at a reciprocal temperature of zero. Now, the slope of each line is

$$\frac{\log(t)-\log(t_a)}{(1/T)-(1/T_a)}. \qquad [7]$$

With the additional assumption that the slope is a linear function of $\log(\sigma)$ (or, equivalently, $\log(\sigma)$ is a linear function of the slope), it follows that:

$$\log(\sigma)=a+b\cdot\left(\frac{\log(t)-\log(t_a)}{(1/T)-(1/T_a)}\right). \qquad [8]$$

This implies:

$$\log(t)=\left(\log(t_a)-\frac{a}{T_a}\right)+a\cdot\left(\frac{1}{T}\right)+\frac{b}{T_a}\cdot\log(\sigma)+b\cdot\log(\sigma)\cdot\left(\frac{1}{T}\right), \qquad [9]$$

which is a generalization of equation 3, in that it includes a linear $\log(\sigma)$ term. This formulation has equivalent flexibility to the Manson-Haferd formulation, but retains the reciprocal temperature dependence. This is illustrated in Figure 3. This parameterization will be denoted as the *Mendelson-Roberts-Manson* (*M-R-M*) parameterization.

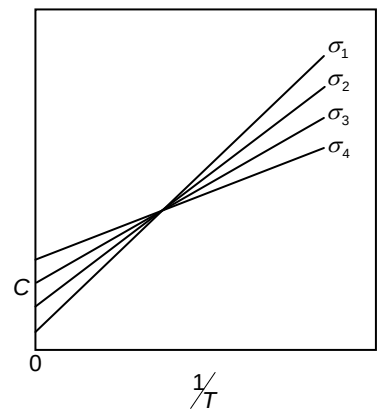

Figure 3. *M-R-M* parameterization.

Like Larson-Miller, the Orr-Sherby-Dorn formulation assumes that $\log(t)$ is a linear function of $1/T$. But, rather than assuming a common intersection of the lines ($\log(t)$, $1/T$) lines, an assumption of <u>no</u> intersection is made (parallel iso-stress lines; see Figure 4).

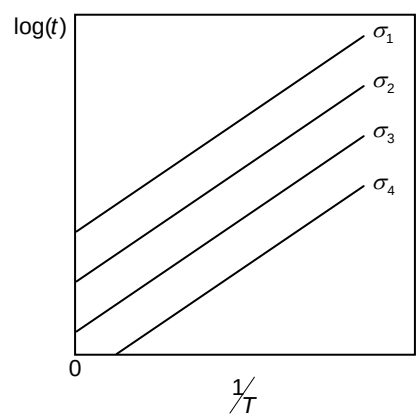

Figure 4. Orr-Sherby-Dorn creep parameterization.

Finally, the Manson-Succop formulation is similar to Manson-Haferd in that straight temperature (vice reciprocal temperature) is used as the predictor of $\log(t)$, but no intersection of the iso-stress lines is allowed (see Figure 5).

Copyright © 2008 by ASME

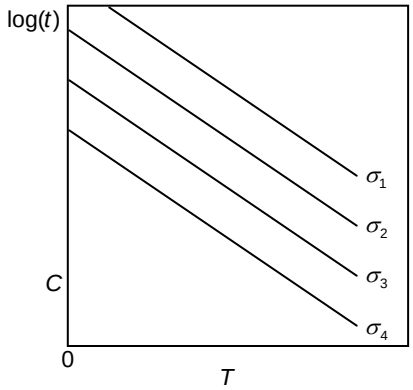

Figure 5. Manson-Succop creep parameterization.

Difficulty in comparing the available model formulations was acknowledged by Conway in Reference 2 (p. 208 – 209), where he notes that preference for the Manson-Haferd approach "might appear to follow from the fact that this parametric approach involves one more constant than employed in the Dorn or Larson-Miller parameters." He continues, "Unfortunately, it is not possible to view a set of stress-rupture data, complete with several isotherms, and tell at a glance which parametric approach would be the best to use." The common framework for data analysis presented in this paper allows for objective, quantitative comparison of the applicability of the different model formulations, which properly accounts for the number of parameters fit in each formulation.

2.0 COMMON GENERAL LINEAR MODEL

As noted above, modeling a material database is often treated as a two-step process, with the first step normalizing the data to an iso-stress condition and the second step fitting a temperature dependence. A more direct view of a creep experiment is as a simple input-output system, in which the inputs are the variables that are controlled by the experimenter, namely temperature and stress, and the output is the measured quantity in the experiment, namely time to rupture or 1% strain. This direct view clarifies the relationship between *applied* experimental conditions and the *measured* response, and suggests the most direct way of applying statistical analysis to the problem of estimating model parameters. Statistical fitting is based on the response variable, t, with the applied conditions (temperature T and applied stress σ) treated as predictor variables in a regression model.

From the results of the last section it can be seen that each of the engineering creep parameterizations is a special case of one of the following linear models:

$$\log_{10}(t) = \beta_0 + \beta_1 \cdot \left(\frac{1}{T}\right) + \beta_2 \cdot \log_{10}(\sigma) + \beta_3 \cdot \log_{10}(\sigma) \cdot \left(\frac{1}{T}\right), \qquad [10]$$

$$\log_{10}(t) = \beta_0 + \beta_1 \cdot T + \beta_2 \cdot \log_{10}(\sigma) + \beta_3 \cdot \log_{10}(\sigma) \cdot T. \qquad [11]$$

The parameters β_0, β_1, β_2, and β_3 can be estimated from creep data, or some of the parameters can be forced to equal zero. Specifically, assuming a power law stress dependence, the common formulations can be interpreted as follows:

- *Larson-Miller* uses Equation 10, with the parameter β_2 fixed at zero;
- *Orr-Sherby-Dorn* uses Equation 10, with the parameter β_3 fixed at zero;
- *Manson-Haferd* uses Equation 11 (no parameters fixed at zero);
- *Manson-Succop* uses Equation 11, with the parameter β_3 fixed at zero.

In addition, the *M-R-M* approach falls into this framework, using Equation 10 with no parameters fixed at zero. This approach allows the same degree of flexibility of the *Manson-Haferd* approach, but with a reciprocal temperature dependence vice a straight linear temperature dependence. This reciprocal temperature dependence may be desirable, since Arrhenius-type, solid state diffusion is involved, even if not rate controlling, in most creep mechanisms.

2.1 Maximum Likelihood Estimation Of Model Parameters

The parameters β_0, β_1, β_2, and β_3 can be estimated from creep data, using the method of maximum likelihood estimation (MLE). This is an established statistical methodology, with well-understood statistical properties based on asymptotic theory (see, e.g., Reference 3). In particular, the MLE method is asymptotically efficient, meaning that for large datasets, no other estimation procedure will yield more precise model parameter estimates. Furthermore, formal quantitative inferences can be made through MLE theory, such as confidence interval estimation of model parameters and hypothesis tests to

Copyright © 2008 by ASME

determine the statistical significance of individual model terms. By comparing the optimized likelihood function for different formulations (based on the different engineering creep parameters), the goodness-of-fit of the formulations can be objectively and quantitatively compared.

MLE has the advantage of readily being able to accommodate censored data, which can occur in two distinct forms. Right-censored data, or *runouts*, are specimens that have not ruptured (or reached the specified 1% strain condition) at the conclusion of the experiment; all that can be stated about such specimens is that their rupture time is longer than the test duration. Left-censored data arise from an experiment in which the lack of in-situ monitoring prevents direct observation of rupture time (or time to 1% strain). If specimens are tested for a fixed time t, and are found to be ruptured at the conclusion of the test, all that can be stated is that their lifetimes were less than the fixed test duration t.

MLE requires that the form of the random variability distribution describing data scatter around the best-estimate creep model be specified (e.g., log-normal, Weibull, etc.). Although this specification is an *a priori* assumption, it can be critically evaluated based on analysis of residuals from the fitted model to ensure that the assumption is warranted for a given database. Standard statistical software is available for fitting linear models via MLE, including the incorporation of censoring. For the analyses presented herein, SAS PROC LIFEREG was used to fit the models and perform statistical inferences. A lognormal probability model was assumed for scatter in the response t; this distribution was subsequently shown to adequately represent the database (as shown in the following section).

In general, maximum likelihood estimation is based on optimizing the likelihood function L, which is defined for a database of n individual specimen tests as

$$L = \prod_{i=1}^{n} L_i\left(t_i;\underline{\theta}\right), \qquad [12]$$

where $\underline{\theta}$ represents a vector of fitting parameters. The estimates of $\underline{\theta}$ are the parameter values that maximize the likelihood function. The contribution to the likelihood function for the ith specimen depends on whether the specimen is an exact time, a right-censored time, or a left-censored time. Specifically,

$$L_i\left(t_i;\underline{\beta}\right) = \begin{cases} f(t_i;\theta) & (\textit{exact time}) \\ 1-F(t_i;\theta) & (\textit{right censored}) \\ F(t_i;\theta) & (\textit{left censored}) \end{cases}, \qquad [13]$$

where $f(t_i, \underline{\theta})$ and $F(t_i, \underline{\theta})$ are the probability density function (PDF) and the cumulative distribution function (CDF) corresponding to the assumed probability model, respectively. For fitting the models of Equation 10 and Equation 11, with a log-normally distributed time response, the PDF is given by

$$\begin{aligned} f(t_i;\underline{\theta}) &= \frac{1}{\sqrt{2\pi}}\frac{1}{\gamma}\exp\left(-\frac{X^2}{2}\right) \\ X &\equiv \frac{1}{\gamma}\left(\begin{array}{l}\log(t_i)-[\beta_0+\beta_1\cdot x+\beta_2\cdot\log_{10}(\sigma) \\ +\beta_3\cdot\log_{10}(\sigma)\cdot x]\end{array}\right) \end{aligned} \qquad [14]$$

where x denotes either temperature T or reciprocal temperature $1/T$, as appropriate, and γ represents the residual standard deviation (which quantifies the data scatter in $\log(t)$ space). The parameter vector $\underline{\theta}$ consists of the regression parameters β_0, β_1, β_2, and β_3, and the residual standard deviation γ. The CDF is given by

$$F(t_i;\underline{\theta}) = \int_{-\infty}^{t_i} f(y;\underline{\theta})\, d\log(y)\,. \qquad [15]$$

In practice, it is numerically more convenient to maximize the natural logarithm of Equation 12; the individual specimens' contributions to the log-likelihood function are additive. The optimized log-likelihood values can be used to compare two models, if one model represents a restriction of the other. Specifically, twice the difference in negative log-likelihood (denoted here as -2LL) is asymptotically distributed as a chi-squared distribution with degrees of freedom equal to the number of parameters fixed in the restricted model relative to the unrestricted model, under the null hypothesis of adequacy of the restricted model to represent the underlying material behavior. The unrestricted model can be considered a statistically significant improvement relative to the restricted model (at the 0.05 level) if the difference in -2LL exceeds the 95th percentile of the chi-squared distribution with the specified degrees of freedom. This procedure will be illustrated in

Copyright © 2008 by ASME

the next sections, which present analysis of two specific material databases.

3.0 APPLICATION TO ALLOY 617

Alloy 617 is a Ni-Cr-Co-Mo alloy that has good high temperature properties, in particular creep strength. It was chosen as the focus of an effort in the early 1980's to draft a Code Case for the ASME Boiler and Pressure Vessel Code, Section III, Elevated Temperature, because it was a leading candidate of designers, and there existed a considerable material properties database at the temperatures of interest. A property data package compiled by Bassford, Reference 4, was used by the ASME Task Force – Very High Temperature Design for the development of the Code Case. The Code Case effort for Alloy 617 was suspended in the late 1980's when the Department of Energy canceled the Very High Temperature Reactor Project and funding for the Code Case effort ceased. The Reference 4 data tables were obtained from the ASME Boiler & Pressure Vessel (B&PV) Committee, Subgroup on Elevated Temperature Design of Subcommittee on Design. The Alloy 617 database contains 173 exact failure time values and 62 right-censored values (specimens for which the test was stopped before rupture was observed).

3.1 Time To Rupture

For the analysis of the Alloy 617 data, the four standard formulations described above were applied. In addition, the *M-R-M* approach was evaluated. Equations 10 and 11 were fit to the data via the method of maximum likelihood estimation. Normally distributed random errors were assumed in $\log_{10}(t)$ space. Comparisons of fit quality among the standard formulations and the *M-R-M* formulation were made using the -2LL criterion. The fitting was done with SAS PROC LIFEREG. The quality of each of the five models considered is summarized in Table 1.

From Table 1, it is apparent that the *M-R-M* model most effectively summarizes the Alloy 617 database. The statistical significance of the improvement in fit of this model relative to the Larson-Miller model (the nearest competitor) can be made based on the improvement in -2LL of the former model relative to the latter. Specifically, -2LL will follow (asymptotically) a chi-squared distribution with one degree of freedom, under the null hypothesis of sufficiency of the Larson-Miller model. The 95th percentile of the chi-squared distribution with one degree of freedom is 3.84; since the observed improvement in -2 log-likelihood afforded by the *M-R-M* model is 8.5, it can be concluded that the *M-R-M* model provides a statistically significant improvement in fit as compared to the Larson-Miller model.

Table 1. Fit Summary for Alloy 617 Time To Rupture

Formulation	Model Form	Parameters Fixed at Zero	log-likelihood*
M-R-M	Eq. [10]	None	-56.74
Larson-Miller	Eq. [10]	β_2	-60.99
Orr-Sherby-Dorn	Eq. [10]	β_3	-129.64
Manson-Haferd	Eq. [11]	None	-76.95
Manson-Succop	Eq. [11]	β_3	-77.71

* Larger (less negative) values indicate better fit to the database.

The fit of the *M-R-M* model is given by:

$$\begin{aligned}\log_{10}(t) = &-20.07 + 37531\cdot\left(\frac{1}{T}\right)\\ &+1.20\cdot\log_{10}(\sigma)\\ &-7568\cdot\log_{10}(\sigma)\cdot\left(\frac{1}{T}\right)\end{aligned} \quad . \qquad [16]$$

This fit is displayed with the database in Figures 6(a) and 6(b). Blue crosses represent exact failure time data; green triangles represent right-censored (lower bound) failure time data.

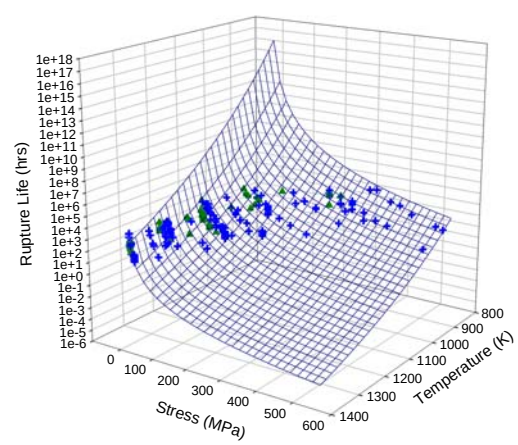

Figure 6(a). Creep rupture life regression model.

Copyright © 2008 by ASME

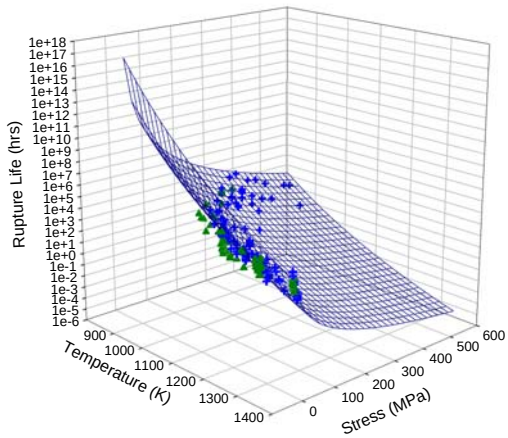

Figure 6(b). Creep rupture life regression model.

Figure 7 displays the measured vs. predicted $\log_{10}$ time to rupture; from this figure, it can be seen that the model fits the data quite well. (It should be noted that the right censored data points are expected to fall – for the most part – below the one-to-one line.) Figure 8 displays a normal probability plot of the residuals from the Equation 16 fit. A normal probability plot is used to assess the adequacy of the normal probability distribution for describing data scatter. Normally distributed data will fall approximately on a straight line in such a plot; of course, due to random variability, actual test data will never fall exactly on a straight line. By evaluating the trend exhibited by the residuals in Figure 8, the normal probability model is judged to approximate the data scatter very well. It is well to remember that in a creep rupture test, the specimen is loaded at temperature until the target applied stress is reached. Then it is held constant at that level until creep rupture occurs. Thus a restriction based on physical consideration needs to be placed on the predictor variable σ in Equation 16; namely that the applied stress needs to be lower than the tensile strength, S_u (otherwise, there will not be any subsequent creep rupture test to be performed).

Lower bound curves for time to creep rupture can be computed based on the fitted model (Equation 3) and the observed variability ("data scatter") in measured times. A lower bound curve should also account for uncertainty in the fitted model parameters. Accounting for uncertainties creates a lower bound that is backed-off from the best estimate $\log_{10}(t)$ by a different amount at different stress-temperature combinations; this is due to the fact that the propagation of uncertainties depends on the degree to which the model is extrapolated relative to the database. However, for simplicity of application, a constant back-off is preferable.

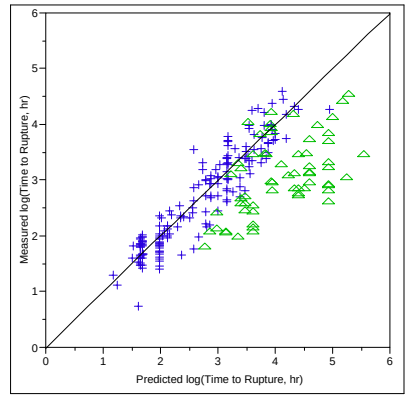

Figure 7. Actual vs. predicted $\log_{10}$(time-to-rupture).

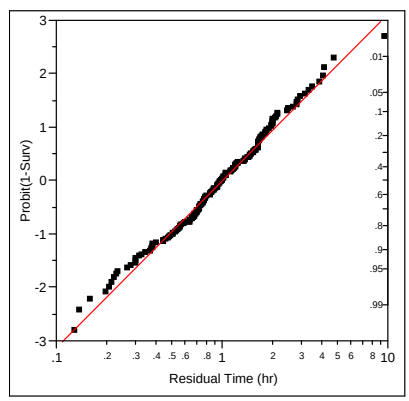

Figure 8. Normal probability plot of the residuals from the regression fit of time to creep rupture.

To support the flight conditions of Project Prometheus the creep model was limited to temperatures between 800 and 1200 K and lifetime extrapolations of no more than 175,000 hours (approximately 20 years). Furthermore, the stress is limited to 500 MPa, which would allow an adequately conservative maximum prediction standard error, subject to the above lifetime and temperature restrictions, to be obtained. It is noted that the creep rupture data cover temperatures in the range 866K to 1366K, and the longest rupture time in the database was 28,735 hours.

Generally, extrapolation of the regression model or the lower prediction bound to combinations of applied stress, temperature and time beyond those represented in the

Copyright © 2008 by ASME

database carries substantial risk, since no empirical validation of the fitted model with actual test data is possible at such conditions. However, some degree of extrapolation will almost surely be required from the accelerated test conditions when the regression model is used for design purposes, as was performed for the interim design curves developed for Project Prometheus pre-conceptual design. The lower bound curves do account for some of the uncertainties, but not necessarily the validity of the fitted model itself, in extrapolating outside of the data range. Care must be exercised to ensure that any required extrapolation yields physically reasonable predictions, if the model is extrapolated far from the database. This is especially true when inverting the model in Equation 16 to predict stress required for a specified time to rupture at a given temperature. In this case, using the tensile strength to set an upper bound on the creep rupture stress, as discussed above, would be recommended.

Over the selected range of time, temperature, and stress described above, the maximum prediction standard error (due to uncertainty in estimated model parameters) is 0.157. This standard error is expressed in $\log_{10}(t)$ space; exponentiation (base 10) converts this back to the raw *time* space as a relative standard error of 2.08x on predicted times. Combined with a residual standard deviation of 0.319 (2.08x in *time*), this yields an overall predictive standard deviation of 0.356 (2.27x in *time*); this is the root-sum-square of the prediction standard error and residual standard deviation. This predictive standard deviation can be applied over the entire restricted range of time, temperature, and stress; it will be slightly conservative at some locations in that space. A $100 \cdot P$ percent lower prediction bound on $\log_{10}(t)$ can be computed as

$$\log_{10}(t) = -20.07 + 37531 \cdot \left(\frac{1}{T}\right) + 1.20 \cdot \log_{10}(\sigma) - 7568 \cdot \log_{10}(\sigma) \cdot \left(\frac{1}{T}\right) - z \cdot 0.356 \qquad [17]$$

where z denotes the $100 \cdot P^{th}$ percentile of the standard normal distribution. Values of z for various coverage probabilities are displayed in the Table 2.

For example, a 95% lower bound on $\log_{10}(t)$ would be computed as

$$\log_{10}(t) = -20.66 + 37531 \cdot \left(\frac{1}{T}\right) + 1.20 \cdot \log_{10}(\sigma) - 7568 \cdot \log_{10}(\sigma) \cdot \left(\frac{1}{T}\right) \qquad [18]$$

If desired, this can be rearranged to form a 95% lower bound on $\log_{10}(\sigma)$ as a function of t and T, as follows:

$$\log_{10}(\sigma) = \frac{\log_{10}(t) + 20.66 - 37531 \cdot \left(\frac{1}{T}\right)}{1.20 - 7568 \cdot \left(\frac{1}{T}\right)}. \qquad [19a]$$

This equation can be rearranged to arrive at the 95% lower bound creep rupture stress, $S_{r,\,min}$, as:

$$S_{r,\min} = \textit{Lesser of} \left\{ 10^{\left(\frac{37531-20.66T}{7568-1.20T}\right)} \cdot t^{\frac{-T}{7568-1.20T}} MPa, S_u \right\}. \qquad [19b]$$

subject to the conditions

$$800\ \text{K} \le T \le 1200\ \text{K}, \quad 0 < t \le 175{,}000 \quad \text{hours}. \qquad [19c]$$

Table 2. Standard Normal Coverage Multipliers

P	z
0.5	0.000
0.75	0.674
0.8	0.842
0.85	1.036
0.9	1.282
0.95	1.645
0.99	2.326

3.2 Time to 1% Strain

For the time to 1% strain response (this is the total mechanical strain which includes elastic and inelastic strains), the Alloy 617 database contains 115 exact failure time values, 18 right-censored values (specimens for which the test was stopped before 1% strain was observed), and 18 left-censored values (specimens for which strains greater than 1% were observed, for which the 1% strain time is not known precisely, but only bounded above). The 18 left-

Copyright © 2008 by ASME

censored values behaved very differently from the remainder of the database, and were excluded from the analysis. Although there is no record of incorrect test method or other issues that call these data into question, their lack of agreement with the remainder of the database is taken as sufficient justification to eliminate them from the analysis. This elimination must be considered as adding risk to the analytical results, in the sense that the fit to the remainder of the database will predict longer times to 1% strain than reported for the left-censored specimens. It should be noted, however, that the left-censored specimens corresponded to high stress levels (in excess of 240 MPa); since it is expected that the creep model may limit performance at low stress levels, this limits the practical impact of the data elimination to some extent. The eliminated data will be discussed further below.

The quality of each of the five models considered is summarized in Table 3. From Table 3, it is apparent that the *M-R-M* model most closely summarizes the behavior of the Alloy 617 database. However, the statistical significance of the improvement in fit of this model relative to the *Orr-Sherby-Dorn* model (the nearest competitor) yields an observed improvement in -2LL of 0.54, which is not statistically significant at the 0.05 level. (That is, the magnitude of this slight improvement in fit can be explained purely by the random variability exhibited by the data.) Therefore, in the interest of making a simpler model and avoiding unnecessary terms in the model (which are undesirable for reasons of practical applicability and numeric stability of parameter estimation), the Orr-Sherby-Dorn model is selected as the most appropriate summary of the observed material behavior.

Table 3. Fit Summary for Alloy 617 Time To 1% Strain

Formulation	Model Form	Parameters Fixed at Zero	log-likelihood*
M-R-M	Eq. [10]	None	-111.35
Larson-Miller	Eq. [10]	β_2	-122.83
Orr-Sherby-Dorn	Eq. [10]	β_3	-111.62
Manson-Haferd	Eq. [11]	None	-116.26
Manson-Succop	Eq. [11]	β_3	-127.00

* Larger (less negative) values indicate better fit to the database.

The fit of the *Orr-Sherby-Dorn* model is given by:

$$\log_{10}(t) = -11.69 + 27018 \cdot \left(\frac{1}{T}\right) - 5.77 \cdot \log_{10}(\sigma) \quad . \qquad [20]$$

The *Orr-Sherby-Dorn* fit is displayed with the database in Figures 9(a) and 9(b). The blue symbols (crosses) represent exact failure time data; the green symbols (triangles) represent right-censored (lower bound) failure time data; the red symbols (inverted triangles) represent left-censored (upper bound) failure time data. It can be seen from these figures that the model provides an unbiased fit to the majority of the database. The left-censored values, which were eliminated from the database for the fitting of Equation 20, are not well predicted. However, Figure 10 shows a different view of this plot, from which it can be seen that several exact failure and right-censored data points fall in the same stress-temperature range as the eliminated left-censored points. The discrepancy between the left-censored points and the remainder of the database therefore cannot be explained by a misspecification of the regression model. The lack of smooth transition between the left-censored points and the remainder of the database was a primary factor in the decision to eliminate those values from the regression modeling. As noted above, this elimination involves some risk, but it is judged to provide the most believable summary of this creep response.

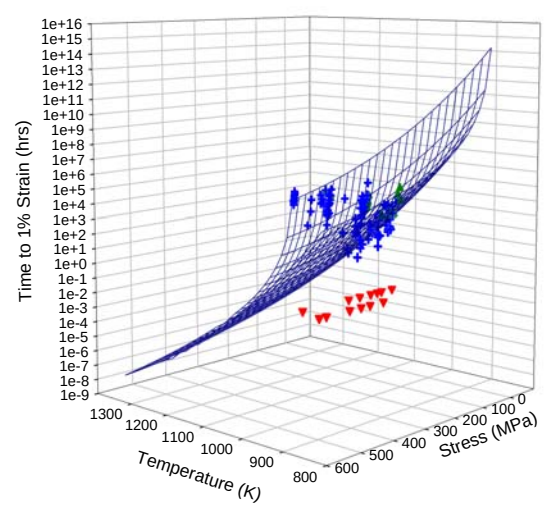

Figure 9(a). Time to 1% creep strain regression model.

Copyright © 2008 by ASME

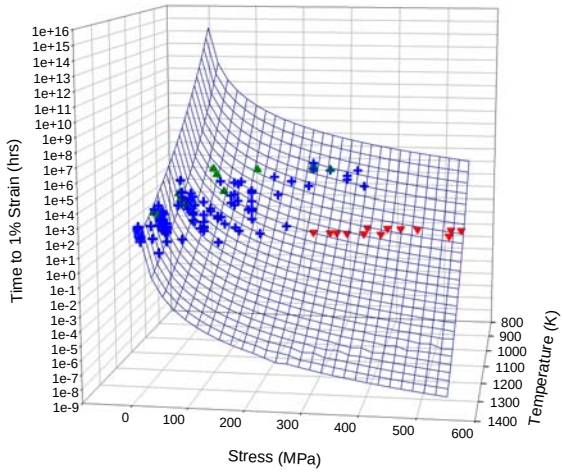

Figure 9(b). Time to 1% creep strain regression model.

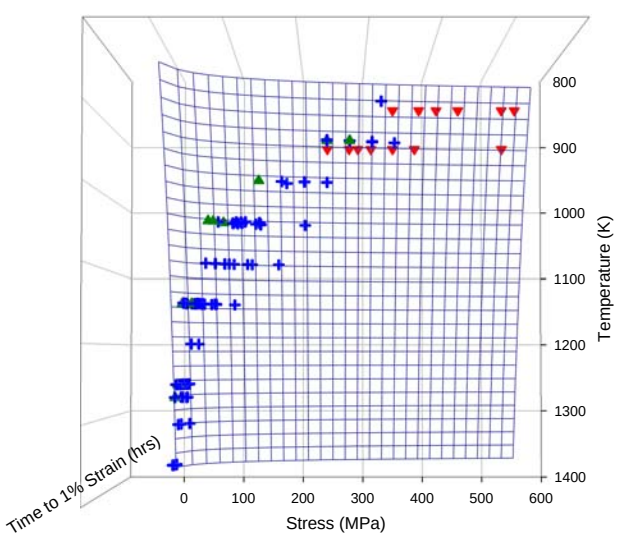

Figure 10. Time to 1% creep strain regression model. functional model form chosen to summarize the data.

Figure 11 displays a plot of measured vs. predicted $\log_{10}$ time to 1% strain. The right-censored points (shown in green) falling largely below the one-to-one line are consistent with the fitted model. The left-censored points (shown in red) are not consistent with the model, as explained above. Figure 12 displays a normal probability plot of the residuals from the fit of Equation 20; based on the approximately linear behavior exhibited in this plot, the normal model is adequate for summarizing the variability observed in the test data.

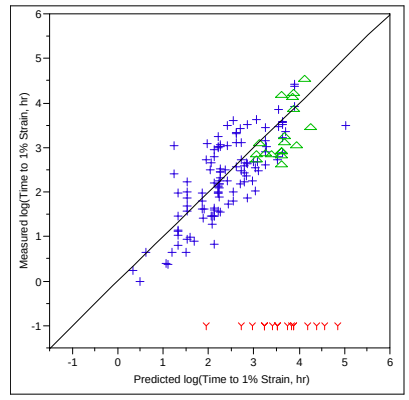

Figure 11. Actual vs. predicted log(time-to-1%-strain).

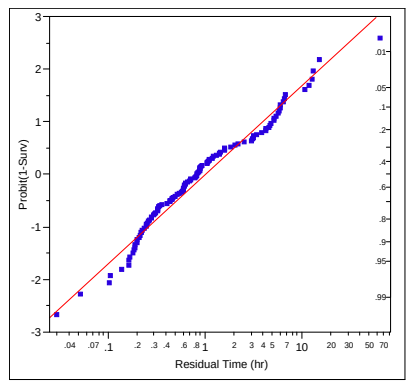

Figure 12. Normal probability plot of the residuals from the regression fit of time to 1% creep strain, excluding the left-censored values.

It is noted that the concept of time to 1% strain under creep condition is not valid when the preload induces an initial strain greater than 1% in the specimen. Thus, a restriction should be placed on the predictor variable σ in Equation 20 such that it is less than the flow stress at 1% total strain, as determined from the stress-strain curve at temperature. Although there is uncertainty as to which flow curve should be used because they are sensitive to strain rates (or stress rates) at very high temperatures, an adequately conservative restriction would be to use the yield strength to restrict the values of σ in Equation 20. A value of 350 MPa is selected to determine the lower bound values of time to 1% strain.

The maximum prediction standard error on $\log_{10}(t)$ over the range 800 K $\leq T \leq$ 1200 K, $t \leq$ 175,000 hours, and $\sigma <$ 350

Copyright © 2008 by ASME

MPa is 0.419 (2.62x in *time*). The residual standard deviation is 0.591 (3.90x in *time*). The combined predictive standard deviation based on these two components is 0.724 (5.30x in *time*). A 100·*P* percent lower prediction bound on $\log_{10}(t)$ can be computed as

$$\log_{10}(t) = -11.69 + 27018 \cdot \left(\frac{1}{T}\right) - 5.77 \cdot \log_{10}(\sigma) - z \cdot 0.724 \quad . \qquad [21]$$

For example, a 95% lower prediction bound on $\log_{10}(t)$ is

$$\log_{10}(t) = -12.88 + 27018 \cdot \left(\frac{1}{T}\right) - 5.77 \cdot \log_{10}(\sigma), \qquad [22]$$

and a lower 95% prediction bound on $\log_{10}(\sigma)$ can be derived as

$$\log_{10}(\sigma) = -\frac{1}{5.77} \cdot \log_{10}(t) - \frac{12.88}{5.77} + \frac{27018}{5.77} \cdot \frac{1}{T} \quad . \qquad [23a]$$

This equation can be rearranged to arrive at the 95% lower bound stress-to-1%-strain, $S_{1\%,\min}$, as:

$$S_{1\%,\min} = \textit{Lesser of} \left\{ 10^{\left(\frac{27018-12.88T}{5.77T}\right)} \cdot t^{\frac{-1}{5.77}} MPa, S_y \right\} . \qquad [23b]$$

subject to the conditions

$$800\ \mathrm{K} \le T \le 1200\ \mathrm{K}, \quad 0 < t \le 175{,}000 \quad \text{hours} \quad . \qquad [23c]$$

The prior explanation of risks of extrapolating the time to rupture model apply equally to the time to 1% strain model (Equation 20) and its associated lower prediction bound (Equation 21). In particular, use of the inverted form, Equation 23, requires careful consideration on the part of the user to ensure that the model does not predict physically unrealistic stresses.

4.0 APPLICATION TO ALLOY 230

4.1 Time to Rupture

A database of Alloy 230 creep test results was obtained from Reference 5. The Alloy 230 database contains 142 exact rupture time values and 75 right-censored values (specimens for which the test was stopped before rupture was observed). The quality of fit of each of the five models considered is summarized in Table 4. From Table 4, it is apparent that the *M-R-M* model most effectively summarizes the Alloy 230 database. The improvement in fit of this model relative to the *Manson-Haferd* model (the nearest competitor) can be made based on the -2LL criterion, as described above. That is, the magnitude of the improvement in fit of the *M-R-M* model relative to the other models is sufficiently large that it cannot be explained purely by the random variability exhibited by the database.

Table 4. Fit Summary for Alloy 230 Time To Rupture

Formulation	Model Form	Parameters Fixed at Zero	log-likelihood*
M-R-M	Eq. [10]	None	25.36
Larson-Miller	Eq. [10]	β_2	-58.66
Orr-Sherby-Dorn	Eq. [10]	β_3	-136.23
Manson-Haferd	Eq. [11]	None	-4.31
Manson-Succop	Eq. [11]	β_3	-75.80

* Larger (less negative) values indicate better fit to the database.

The fit of the *M-R-M* model is given by:

$$\log_{10}(t) = -26.27 + 44158 \cdot \left(\frac{1}{T}\right) + 4.72 \cdot \log_{10}(\sigma) - 11337 \cdot \log_{10}(\sigma) \cdot \left(\frac{1}{T}\right) \qquad [24]$$

This fit is displayed with the database in Figure 13. Figure 14 displays the measured vs. predicted $\log_{10}$ time to rupture; from this figure, it can be seen that the model fits the data quite well. Figure 15 displays a normal probability plot of the residuals from the Equation 24 fit; based on this plot, the normal probability model can be seen to approximate the data scatter reasonably well. Figure 16 displays the residuals from the fit against one of the two predictor variables in the model, namely $\log_{10}(\sigma)$; from this figure, it can be observed that there is some lack-of-fit in the stress dependency of the fitted model (Equation 24). In particular, there appears to be some nonlinearity in the residual plot. Although it would be possible to formulate a regression

Copyright © 2008 by ASME

model form more general than any summarized in Table 4, there would be considerable risk in extrapolating such a model to lower stresses. Therefore, the model of Equation 24 is recommended, despite its slight deficiencies.

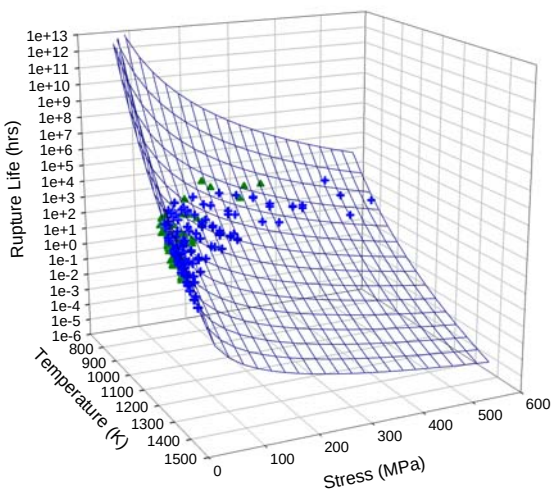

Figure 13. Creep rupture life regression model.

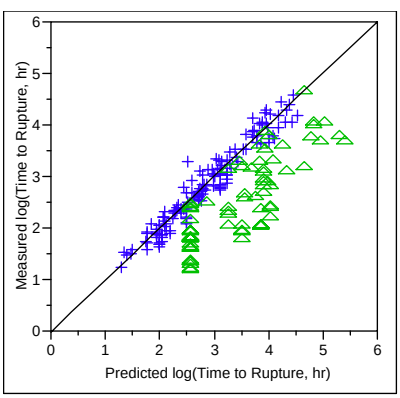

Figure 14. Actual vs. predicted $\log_{10}$(time-to-rupture).

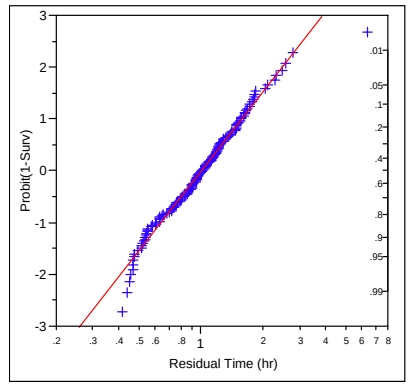

Figure 15. Normal probability plot of the residuals from the regression fit of time to creep rupture.

Similarl to the consideration for the Alloy 617 database, a 95% lower prediction bound on $\log_{10}$(rupture time), subject to the conditions of 800 K $\leq T \leq$ 1200 K, $0 < t \leq$ 175,000 hr, $\sigma \leq$ 500 MPa, is given as

$$\log_{10}(t) = -26.64 + 44158 \cdot \left(\frac{1}{T}\right) + 4.72 \cdot \log_{10}(\sigma) - 11337 \cdot \log_{10}(\sigma) \cdot \left(\frac{1}{T}\right) \quad [25a]$$

This equation can be rearranged to arrive at the 95% lower bound creep rupture stress, $S_{r,\,min}$, as:

$$S_{r,\min} = \textit{Lesser of} \left\{ 10^{\left(\frac{44158-26.64T}{11337-4.72T}\right)} \cdot t^{\frac{-T}{11337-4.72T}} MPa, S_u \right\}. \quad [25b]$$

with the conditions

$$\begin{array}{c} 800\text{ K} \leq T \leq 1200\text{ K}, \\ 0 < t \leq 175{,}000 \quad \text{hours} \end{array}. \quad [25c]$$

The magnitude of the selected offset does lower bound the majority of the residuals displayed in Figure 16 (the purple symbols), so the lower bound is considered appropriately conservative in spite of the model deficiencies. The majority of the ruptured specimens would be bounded by a 95% lower prediction bound (which would appear on this plot as a horizontal line at a height of approximately *residual* = – 0.37). It is noted that the creep rupture data

Copyright © 2008 by ASME

cover temperatures in the range 866K to 1422K, and the longest rupture time in the Alloy 230 database was 39,044 hours.

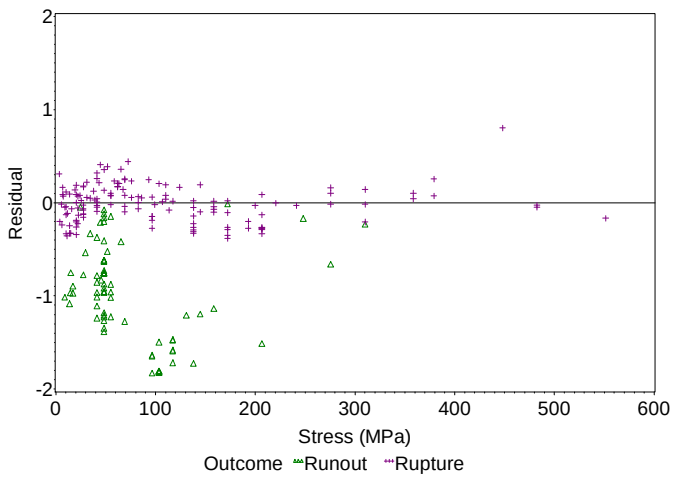

Figure 16. Residuals from the rupture fit vs. applied stress.

4.2 Time to 1% Strain

The Alloy 230 database contains 199 exact time-to-one-percent-strain values and 18 right-censored values (specimens for which the test was stopped before 1% strain was observed).

The quality of fit of each of the five models considered is summarized in Table 5. Comparing the log-likelihood values from Table 5, it is apparent that the *M-R-M* model most closely summarizes the behavior of the Alloy 230 database. The *Manson-Haferd* model is a close competitor, but is not as effective as the *M-R-M* model for this database.

Table 5. Fit Summary for Alloy 230 Time to 1% Strain

Formulation	Model Form	Parameters Fixed at Zero	log-likelihood*
M-R-M	Eq. [10]	None	-142.05
Larson-Miller	Eq. [10]	β_2	-156.29
Orr-Sherby-Dorn	Eq. [10]	β_3	-201.86
Manson-Haferd	Eq. [11]	None	-144.09
Manson-Succop	Eq. [11]	β_3	-171.41

* Larger (less negative) values indicate better fit to the database.

The fit of the *M-R-M* model is given by:

$$\log_{10}(t) = -21.78 + 37336 \cdot \left(\frac{1}{T}\right) + 3.16 \cdot \log_{10}(\sigma) - 9320 \cdot \log_{10}(\sigma) \cdot \left(\frac{1}{T}\right) \quad .[26]$$

This fit is displayed with the database in Figure 17. Figure 18 displays the measured vs. predicted $\log_{10}$ time to rupture; from this figure, it can be seen that the model fits the data reasonably well. However, there is considerably more scatter in the data than was the case for the rupture time model for this material presented previously. Figure 19 displays a normal probability plot of the residuals from the Equation 25 fit; based on this plot, the normal probability model can be seen to approximate the data scatter reasonably well. Figures 20(a) and 20(b) display the residuals from the fit against $\log_{10}(\sigma)$ and temperature (K). Lack-of-fit is evident in these residual plots, similar in character to that displayed by the rupture time fit, but considerably greater in magnitude. As with the rupture time fit, the *M-R-M* model is recommended, despite its deficiencies. Again, this is because no other functional form is known that could summarize the data more effectively and be relied upon to extrapolate reasonably to lower stress values.

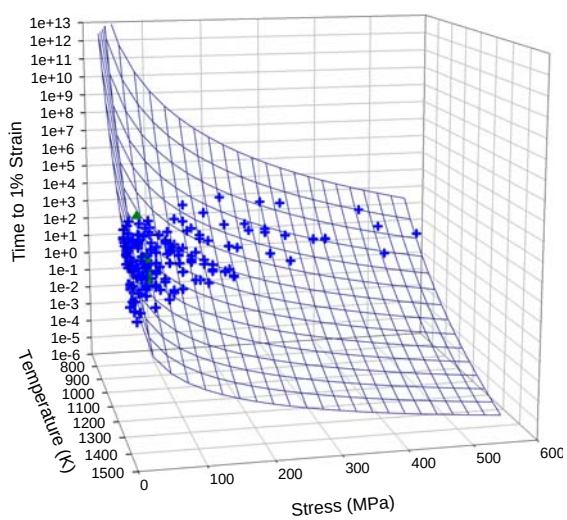

Figure 17. Time to 1% total strain regression model.

Copyright © 2008 by ASME

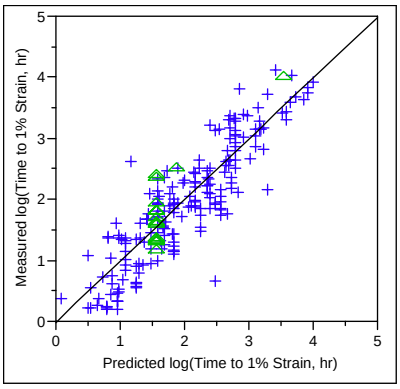

Figure 18. Actual vs. predicted $\log_{10}$(time-to-1%-strain).

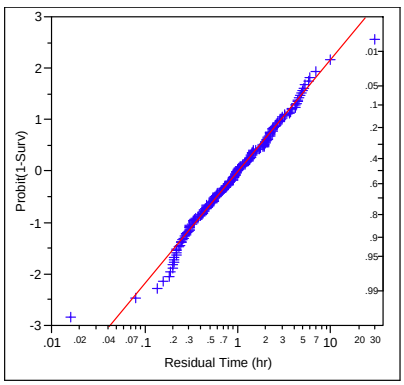

Figure 19. Normal probability plot of the residuals from the regression fit of time to 1% total strain.

Similar to the consideration for the Alloy 617 database, a 95% lower prediction bound on the time to 1% strain (in $\log_{10}$ space), subject to the conditions of 800 K $\leq T \leq$ 1200 K, $0 < t \leq 175{,}000$ hr, $\sigma \leq 400$ MPa, is given as

$$\log_{10}(t) = -22.60 + 37336 \cdot \left(\frac{1}{T}\right) + 3.16 \cdot \log_{10}(\sigma) - 9320 \cdot \log_{10}(\sigma) \cdot \left(\frac{1}{T}\right) \quad [27a]$$

This equation can be rearranged to arrive at the 95% lower bound stress-to-1%-strain, $S_{1\%,\min}$, as:

$$S_{1\%,\min} = \textit{Lesser of} \left\{ 10^{\left(\frac{37336-22.60T}{9320-3.16T}\right)} \cdot t^{\frac{-T}{9320-3.16T}} MPa, S_y \right\}. \quad [27b]$$

subject to the conditions

$$800\text{ K} \leq T \leq 1200\text{ K}, \quad 0 < t \leq 175{,}000 \quad \text{hours}. \quad [27c]$$

The selected magnitude of offset does lower bound the majority of the residuals displayed in Figure 20 (the purple symbols), so the lower bound is considered appropriately conservative in spite of the model deficiencies. The majority of the ruptured specimens would be bounded by a 95% lower prediction bound, which would appear on these residual plots as a horizontal line at a height of approximately –0.82. An exception to this is combinations of temperature greater than 1300 K and stress less than 20 MPa, where some observed times to 1% strain were less than the 95% lower prediction bound.

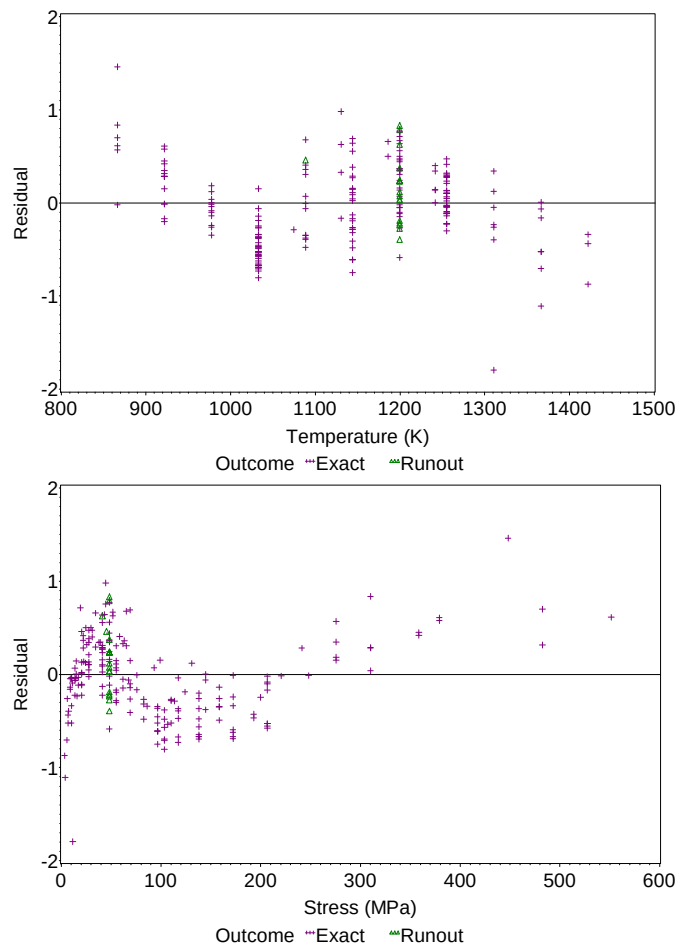

Figure 20. Residuals from the 1% strain fit vs. temperature (upper), and applied stress (lower).

Copyright © 2008 by ASME

5.0 REASONABLENESS OF PARAMETERS

While the *M-R-M* approach is empirical, the equation form encompasses both an apparent activation energy term: $\beta_1 \cdot (1/T)$, as well as a stress-activation energy interaction term: $\beta_3 \cdot \log_{10}(\sigma) \cdot (1/T)$. Realistic activation energies lend confidence to these extrapolations and can give some insight into the mechanism or mechanisms that control creep damage. In order to assess the reasonableness of the *M-R-M* method, the minimum and maximum apparent activation energies were estimated for both the Alloy 617 and Alloy 230 failure data, using the minimum and maximum stresses in the database. As shown in Table 6, the maximum apparent activation energies for creep in both Alloy 617 (262 kJ/mol) and Alloy 230 (322 kJ/mol) are consistent with either the self diffusion of nickel (~290 kJ/mol) or some slow diffusing solute (e.g. tungsten diffusion in nickel with an activation energy of ~299 kJ/mol). The apparent activation energies are decreased as the applied stress increases, but even at the highest levels tested (~ 550MPa), they remain positive and physically realistic.

Table 6. Comparison of the Apparent Activation Energies for Creep and Substitutional Diffusion in Ni

	Apparent Activation Energy (kJ/mol)		Reference
	Maximum	Minimum	
IN 617	262	140	This Work
Haynes 230	322	108	This Work
Ni Self Diffusion	290		[6]
W Diffusion in Ni	299		

5.1 Comparisons

In Section II, Part D, Subpart 1B of the ASME B&PV Code, Reference 7, the maximum allowable stress values, S, for Alloy 617 and Alloy 230 are tabulated for Section I and Section VIII, Division 1 applications for non-nuclear components. The S values are determined, per the Mandatory Appendix 1 of Reference 7, as the smallest of:

- 100% of the average stress to produce a creep rate of 0.01%/1,000 hr
- 100% of the average stress to cause rupture at the end of 100,000 hr
- 80% of the minimum stress to cause rupture at the end of 100,000 hr

Although there is no indication in the stress tables as to which of the three criteria controls the S value at a specific temperature, it is generally considered that 80% of the minimum creep rupture strengths at 100,000 hours governs the S values at higher temperatures. Figure 21 compares the values of $S_{r,\,min}$ for Alloy 617 from Equation 19b at 100,000 hours to those from the Stress Tables of Reference 7. The minimum creep rupture strengths at 100,000 hours from the Draft Alloy 617 Code Case, Reference 8, are also shown in Figure 21. The comparison is quite good, particularly at high temperatures. Similar comparison is shown in Figure 22 for Alloy 230 and they compare reasonably well at high temperatures.

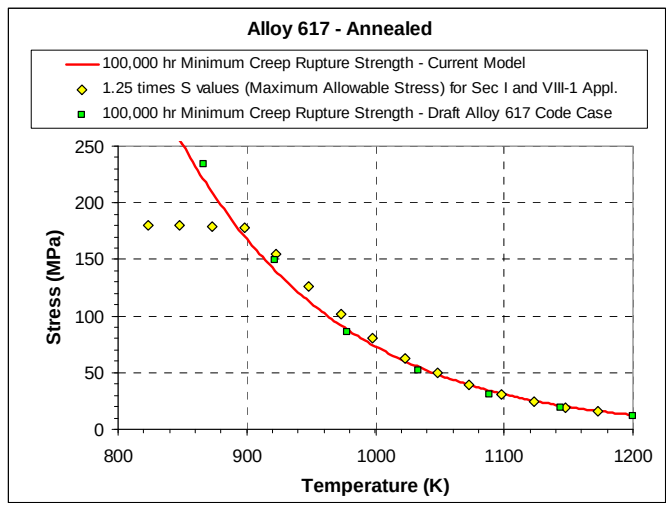

Figure 21. Alloy 617. Comparison of (i) 100,000 hour 95% lower bound creep rupture strength from the present work; (ii) 1.25 times maximum allowable stress value (S) from ASME B&PV Code for Section I and Section VIII Div 1 applications, and (iii) 100,000 hour minimum creep rupture strength from Alloy 617 Draft Code Case.

Copyright © 2008 by ASME

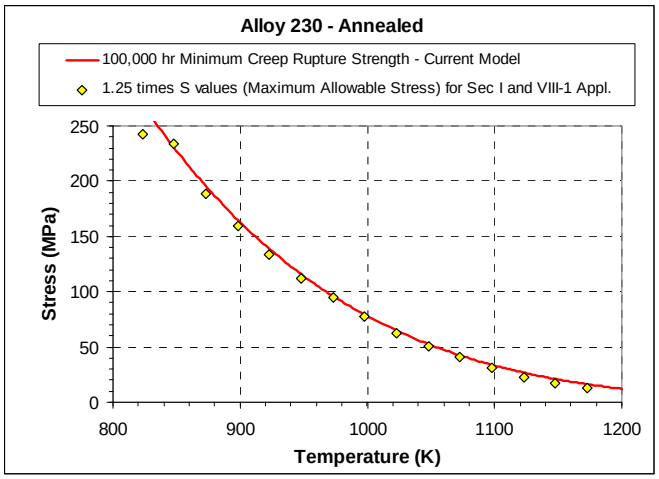

Figure 22. Alloy 230. Comparison of (i) 100,000 hour 95% lower bound creep rupture strength from the present work, and (ii) 1.25 times maximum allowable stress value (*S*) from ASME B&PV Code for Section I and Section VIII Div 1 applications.

6.0 CONCLUSIONS

By viewing engineering creep parameters within the framework of a common underlying statistical framework, many advantages are realized. The models can be fit to a database in a statistically efficient way, and compared to one another with objective and quantified statistical procedures. Censored data can be accommodated in a straightforward and rigorous way. The question of the appropriate form of the temperature dependence (straight temperature or reciprocal temperature) can be separated from the question of interaction between stress and temperature dependencies. However, reciprocal temperature fits for Alloy 617 and Alloy 230 give reasonable apparent activation energies. Probabilistically interpretable lower bounds can be generated from the fitted models. These advantages have been illustrated with application to the commercial materials Alloy 617 and Alloy 230.

REFERENCES

1. Boyer, HE. *Atlas of Creep and Stress-Rupture Curves*. ASM International. 1988.

2. Conway, JB. *Stress Rupture Parameters: Origin, Calculation, and Use*. Gordon and Breach. 1969.

3. Bickel, PJ & Doksum, KA. *Mathematical Statistics: Basic Ideas and Selected Topics*. Prentice Hall. 1977.

4. Bassford, TH, "INCONEL Alloy 617 Data Package Compilation," INCO Alloys International – Huntington. June 1982.

5. Katcher, M, "Haynes 230 creep database in Excel spreadsheet," Haynes International, Inc. 2005

6. J. Askill, Tracer Diffusion Data for Metals, Alloys, and Simple Oxides, Plenum Press, New York, 1970

7. ASME Boiler & Pressure Vessel Code, Section II, Part D Properties (Metric) Materials, 2007 Edition, The American Society for Mechanical Engineers, New York, New York. 2007

8. ASME Boiler & Pressure Vessel Code, Draft Alloy 617 Code Case, Subgroup on Elevated Temperature Design, Task Force – Very High Temperature Design, 1988

Copyright © 2008 by ASME